

The Large-area Hybrid-optics CLAS12 RICH Detector: Tests of Innovative Components

M. Contalbrigo^a, N. Baltzell^k, F. Benmokhtar^h, L. Barion^a, E. Cisbani^c, A. El Alaoui^{k,i}, K. Hafidi^k, M. Hoek^{g,j}, V. Kubarovsky^f, L. Lagamba^d, V. Lucherini^b, R. Malaguti^a, M. Mirazita^b, R. Montgomery^{g,b}, A. Movsisyan^a, P. Musico^e, D. Orecchini^b, A. Orlandi^b, L. L. Pappalardo^a, S. Pereira^b, R. Perrino^d, J. Phillips^g, S. Pisano^b, P. Rossi^{f,b}, S. Squerzanti^a, S. Tomassini^b, M. Turisini^{i,a}, A. Viticchiè^b

^aINFN Sezione di Ferrara and University of Ferrara, Italy

^bINFN Laboratori Nazionali di Frascati, Italy

^cINFN Sezione di Roma - Gruppo Collegato Sanità and Italian National Institute of Health

^dINFN Sezione di Bari and University of Bari, Italy

^eINFN Sezione di Genova, Italy

^fThomas Jefferson National Laboratory, VA USA

^gGlasgow University, UK

^hChristopher Newport University, VA USA and Duquesne University, PA USA

ⁱUniversidad Tecnica Federico Santa Maria, Valparaíso, Chile

^jJ. Gutenberg Universität, Mainz, Germany

^kArgonne National Laboratory, IL USA

Abstract

A large area ring-imaging Cherenkov detector has been designed to provide clean hadron identification capability in the momentum range from 3 GeV/c to 8 GeV/c for the CLAS12 experiments at the upgraded 12 GeV continuous electron beam accelerator facility of Jefferson Lab to study the 3D nucleon structure in the yet poorly explored valence region by deep-inelastic scattering, and to perform precision measurements in hadronization and hadron spectroscopy. The adopted solution foresees a novel hybrid optics design based on an aerogel radiator, composite mirrors and densely-packed and highly-segmented photon detectors. Cherenkov light will either be imaged directly (forward tracks) or after two mirror reflections (large angle tracks). The preliminary results of individual detector component tests and of the prototype performance at test-beams are here reported.

Keywords: Cherenkov radiation, Multi-anode photomultipliers, Silicon photomultiplier, proximity-focusing RICH, Aerogel

1. Introduction

Jefferson Lab (JLab) (VA, USA) is currently undergoing an upgrade program which involves the doubling of the energy of its electron beam from 6 GeV to 12 GeV and the enhancement of detector capabilities in the existing experimental halls. In Hall B, the CLAS12 detector will receive polarised beams of maximum energy 11 GeV and luminosity up to $10^{35} \text{ cm}^{-2}\text{s}^{-1}$, providing a world-leading facility for the study of electron-nucleon scattering with nearly full angular coverage [1]. The physics program is extremely broad [2] but, in particular, will focus upon 3D imaging of the nucleon through the mapping of generalized and transverse momentum dependent parton distributions at unprecedented high Bjorken x [3]. In particular three approved experiments demand an efficient hadron identification across the entire momentum range from 3 to 8 GeV/c and scattering angles up to 25 degrees. A pion rejection power of about 1:500 is required to limit the pion contamination in the kaon sample to a few percent level. The CLAS12 baseline comprises a time-of-flight system (TOF), able to efficiently identify hadrons up to a momentum of about 3 GeV/c, and two Cherenkov gas detectors of high (HTCC) and low (LTCC) threshold, reaching the needed pion rejection power only close to the upper limit (around 7 GeV/c) of hadron momenta and

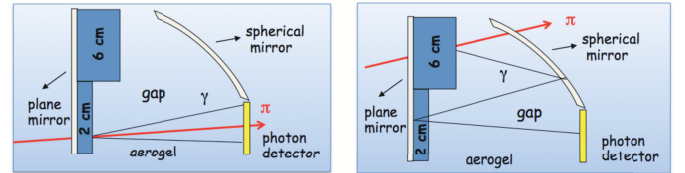


Figure 1: The CLAS12 hybrid optics design (see text for details).

are not able to distinguish kaons from protons. A ring-imaging Cherenkov detector (RICH) has been proposed, replacing at least two symmetric LTCC radial sectors out of the total six, to achieve the needed hadron identification and accomplish the physics program. The radial sectors have a projective geometry, a gap depth of 1.2 m and about 5 m^2 entrance window area. Simulation studies favor a hybrid imaging RICH design incorporating aerogel radiators, visible light photon detectors, and a focusing mirror system [4, 5].

The focusing mirror system will be used to reduce the detection area instrumented by photon detectors to about 1 m^2 per sector, minimizing costs and influence on the detectors (TOF and Calorimeters) positioned behind the RICH, see Fig. 1. For forward scattered particles ($\theta < 13^\circ$) with momenta $p = 3 - 8$

GeV/c, a proximity imaging method with thin (2 cm) aerogel and direct Cherenkov light detection will be used. For larger incident particle angles of $13^\circ < \theta < 35^\circ$ and intermediate momenta of $p = 3 - 6$ GeV/c, the Cherenkov light will be focused by a spherical mirror, undergo two further passes through the thin radiator material and a reflection from planar mirrors before detection. The longer path of light and the focusing mirror allow the use of thick (6 cm) aerogel to compensate yield losses in the thin radiator.

2. The RICH Component Tests

2.1. Aerogel Radiator

The best radiator for RICH hadron identification in the few GeV momentum range is silica aerogel, an amorphous solid network of SiO_2 nanocrystals with a very low macroscopic density and a refractive index in between gases and liquids. It has been successfully used as radiator material for RICH detectors in several particle physics experiments [6] and is planned for future use [7]. A systematic characterization has been carried out in laboratory and during test beams on a variety of aerogel samples from different producers and refractive indexes in the range $n=1.04-1.06$ identified to provide sufficient photon yield. The aerogel from the Budker and Boreskov Catalysis Institutes of Novosibirsk [8] has been studied most thoroughly, because it combines high-transparency with flexibility in geometrical parameters (area and thickness).

Precise measurements of the aerogel transmittance as a function of the wavelength have been performed using a Lambda 650 S PerkinElmer spectrophotometer. During prototyping, the production technique and the resulting quality of the Russian aerogel has been significantly improved with time. Presently, a clarity of the order of $0.0050 \mu\text{m}^4\text{cm}^{-1}$ for a $n=1.05$ refractive index has been achieved, a value comparable with the best ones obtained at lower refractive indexes [9].

In order to study the chromatic dispersion, estimated to be among the largest contributions to the Cherenkov angle resolution, one needs precise measurements of the aerogel refractive index as a function of the wavelength. Different methods were employed, see Fig. 2. The prism method allows to measure the refractive index through the Snell-Descartes formula [10]. The measurements were performed using a monochromatic beam extracted from the spectrophotometer, focused by a series of lenses and recorded by a CCD camera. As a second method, the dependence of the refractive index on the photon wavelength has been studied by applying optical filters just after the $n=1.05$ aerogel radiator in a RICH prototype tested with a 8 GeV/c pion beam (see next Section). The set of available filters allowed to span the entire range of relevant wavelengths, from 300 to 650 nm, in steps of 50 nm. At the reference wavelength of 400 nm, the measured $n = 1.0492 \pm 0.0004$ refractive index (the error is only statistical) is in agreement with the value derived from the known aerogel density of $\rho = 0.230 \text{ g/cm}^3$ and the relation $n^2 = 1 + 0.438\rho$. The data points are consistent with the dispersion model used as input to the RICH simulations, in which the aerogel refractive index is derived as a combination

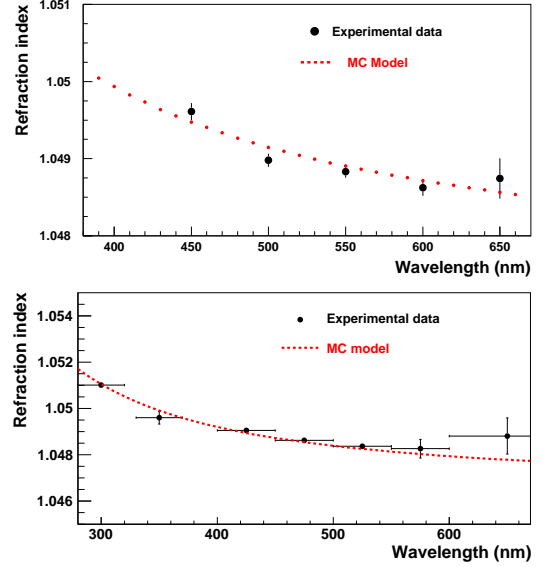


Figure 2: Aerogel dispersion measured with the spectrometer beam and the prism method (top) and with the RICH prototype and 8 GeV/c pion beam by using optical filters (bottom) on two different $n=1.05$ aerogel tiles. The data points are compared with the dispersion model used in input to the RICH Monte Carlo simulations (dashed line).

of its air and quartz components [11]. Due to local inhomogeneities, the refractive index can change significantly (up to $\delta n \approx 10^{-3}$) throughout the tile. The prism method allows to determine the refractive index only in the proximity of the tile edges, whereas the test-beam measurements are time consuming. A complementary approach has been commissioned based on the gradient method [12]. Preliminary results indicate that inhomogeneities contribute to the Cherenkov angle resolution much less than the chromatic dispersion.

2.2. Photon Detector

As confirmed by simulation studies [4], the photon detector must provide a spatial resolution of less than 1 cm not to degrade the Cherenkov angle resolution in the CLAS12 RICH geometry. The Hamamatsu H8500 multianode photomultiplier tubes (MA-PMTs) have been selected as a candidate being an effective compromise between detector performance and cost. It comprises an 8×8 array of pixels, each with dimensions $5.8 \text{ mm} \times 5.8 \text{ mm}$, into an active area of $49.0 \text{ mm} \times 49.0 \text{ mm}$ with a very high packing fraction of 89%. The device offers a spectral response matching the spectrum of light transmitted by the aerogel, with a quantum efficiency peaking at 400 nm, and a fast response (less than 1 ns rise time) useful to suppress background.

Although the H8500 MA-PMT is not advertised as the optimal device for single photon detection purposes, several units have been characterized in laboratory tests and used in test-beams of RICH prototypes with dedicated electronics, achieving performances adequate to the CLAS12 RICH requirements. The uniformity of the H8500 response has been extensively studied with a pico-second pulsed laser. The typical gain vari-

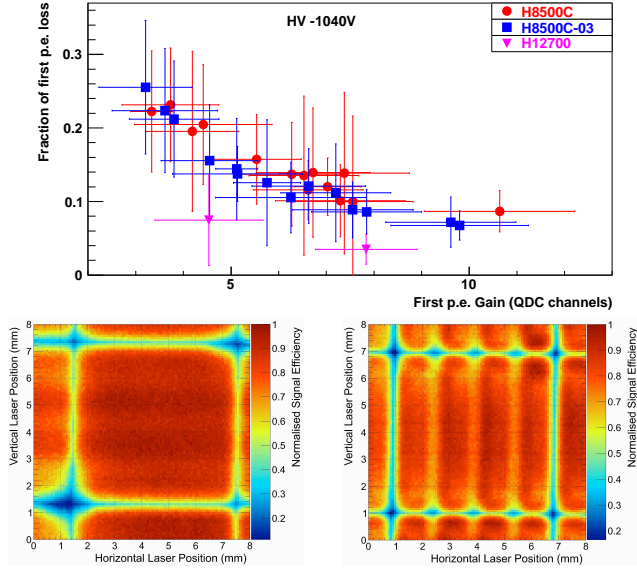


Figure 3: Top: Average fraction of single photoelectron signal losses as a function of the average gain for different MA-PMTs operated at 1040 V and illuminated by a 405 nm laser wavelength. Two H12700 demonstrators are compared to a sample of 28 H8500 MA-PMTs. Bottom: Normalized response map of a H8500 (left) and a H12700 (right) MA-PMT, obtained by scanning a 8×8 mm² area with a pico-second pulsed laser spot of 90 μ m diameter and 635 nm wavelength with step size of 80 μ m.

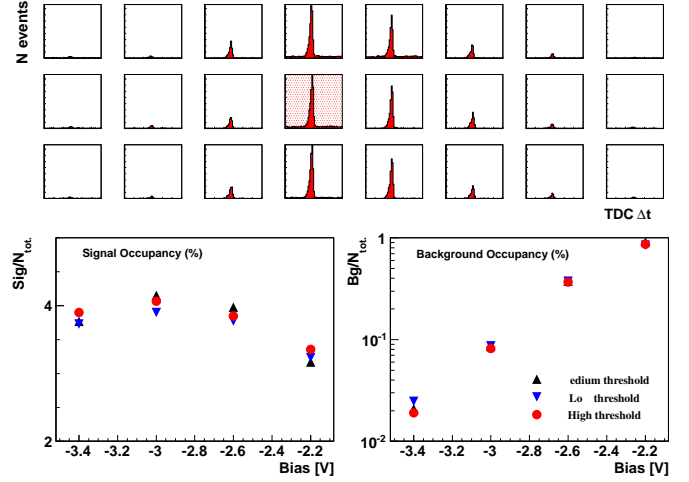


Figure 4: Online results of one of the custom made MPPC matrices operated at -25 degrees. The time difference between any MPPC hit and the trigger (within a 30 ns window) is shown in the top plot for all the pixels. The signal and background occupancies (hits over triggers ratio) in a 3 ns time coincidence within the trigger are shown for pixel 75 (highlighted in the top plot) in the bottom plots, respectively, as a function of the bias voltage and for different discriminator thresholds. The bias voltage is referred to the nominal value at 25 degrees of 72.8 Volt.

ations in the pixel response, of the order of 1:2, can be easily compensated by the readout electronics. Sub-mm precision scans are used to study the PMT response in dead space areas and to evaluate the true active areas of the pixels [13]. Further characterization tests performed include: crosstalk studies, where magnitudes of less than 5% are extracted with both blue and red laser wavelengths, and the fraction of single photoelectron signal lost below the pedestal threshold, which is minimized to less than 15% through operation at 1040V high voltage or above, see Fig. 3. In view of possible future upgrades, two demonstrators of a novel H12700 multi-anode PMT, with the same layout as the H8500 but optimized dynode structure, has been tested yielding promising results in terms of single photon resolution, see Fig. 3.

The fast developing silicon photomultipliers represent a possible cost-effective alternative for future upgrades of the detector. A small prototype was used to study the performance of a 3×3 mm² silicon multi-pixel photon counter (MPPC) matrices with a 3 cm $n=1.05$ aerogel and 36 cm gap. A commercial 8×8 MPPC matrix was compared to two customized 8×4 MPPC matrices with an embedded pre-amplification stage. All the matrices were temperature controlled by means of water cooled Peltier cells. The response to Cherenkov light was studied within a temperature interval ranging from 25 down to -25 degrees Celsius. The MPPC signal hits were selected by a relatively broad trigger time coincidence of ± 3 ns, driven by the external trigger jitter. This limited the dark count background rejection at high temperature, where the working point had to be carefully selected for each pixel in order to optimize and equalize the matrix response. At low temperature, a much

more stable and uniform response could be achieved in a large interval of bias voltage and discriminating threshold values: a 30-40% higher than H8500 single photon detection efficiency was recorded while approaching a manageable 10^{-4} dark count background occupancy, see Fig. 4.

3. The large-size RICH Prototype

Testbeam studies of a large-size prototype RICH detector were performed at the T9 beam line in the CERN-PS East Area, with a mixed hadron beam of 6-8 GeV/c momentum. Two gaseous electron multipliers chambers with 10×10 cm² area and readout in 256 strips for both x and y were used for beam particle tracking. A threshold Cherenkov CO₂ gas counter, part of the T9 beam area equipment, was used to tag pions.

Two setups were mounted inside a large (approximately $1.6 \times 1.8 \times 1.6$ m³) light-tight box to study direct and reflected light imaging modes individually. The Cherenkov light was detected by a circular array of 28 MA-PMTs, alternated of the type H8500C with normal glass and H8500C-03 with UV glass for systematic studies. The MA-PMTs were mounted on a circular support and could be radially moved to intercept the Cherenkov ring produced with different opening angles depending on the chosen refractive index. The prototype readout electronics was based on the MAROC3 [14] chip and derived from medical imaging applications. Each 5×5 cm² front-end MAROC card served a 64 channel multi-anode PMT. The controller board could host up to 64 Front-End cards allowing to concentrate thousands of readout channels in a very compact layout.

The direct light case reproduces the 1 m gap of the CLAS12 geometry, see Fig. 5. In the early stages of data analysis, an average yield of 12 photo-electrons and a π/K separation close

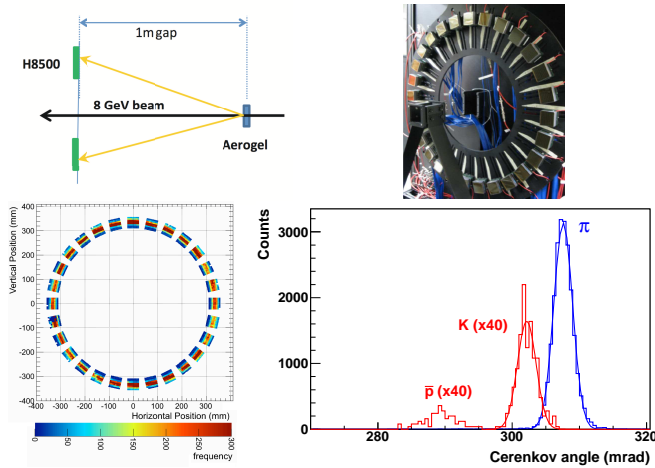


Figure 5: Direct light configuration of the test beam prototype. Top left: Side view diagram illustrating the setup. Top right: Photo of the detector plane. Bottom left: The Cherenkov ring coverage is about 80% for a $n=1.05$ refractive index. Bottom right: Cherenkov angle distributions for 8 GeV/c pions tagged by the T9 gas Cherenkov compared with those of kaons and protons.

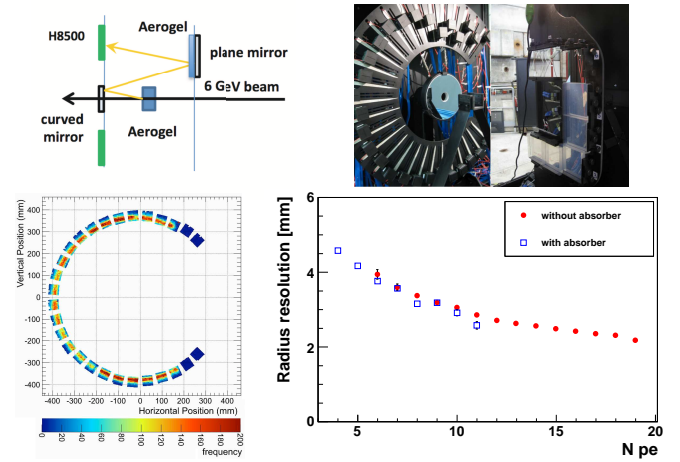


Figure 6: Reflected light configuration of the test beam prototype. Top left: Side view diagram illustrating the setup. Top right: Photo of the detector plane together with the spherical mirror, and of the plane mirror array partially covered by the aerogel tiles. Bottom left: The Cherenkov ring coverage is 60% for a $n=1.05$ refractive index. Bottom right: Cherenkov radius resolution as a function of the photo-electron number for the two cases with and without absorber (aerogel) in front of the planar mirrors.

to the goal value of 4σ in units of Cherenkov angle resolution have been obtained with a 2 cm $n=1.05$ aerogel up to the maximum beam momentum of 8 GeV/c. A better performance is anticipated for the final detector by increasing the MA-PMT ring coverage and using a uniform sample of MA-PMTs with the same type of glass window. Several aerogel thicknesses, transparencies and refractive indexes (in the range 1.04-1.06) were tested and their corresponding impact on the RICH prototype performance are under study for further optimization.

The main aim of the reflected light case was the study of the concept of double reflection with multiple passes through the aerogel, in particular investigating the Cherenkov light yield loss and the contributions to the Cherenkov angle resolution. The prototype allowed to test all the optical components and validate their Monte Carlo description, even though the geometrical constraints of the prototype did not allow to reproduce the CLAS12 reflected light path length and to put the MA-PMTs on the mirror focal plane, see Fig. 6. The Cherenkov light produced by a 6 cm thick $n=1.05$ aerogel were first reflected by a spherical mirror with focal length of 0.9 m and then by a circular array of eight 11.5×11.5 cm² planar mirrors towards the MA-PMTS wall. The supports of the planar mirrors are designed to allow the insertion of 2 cm thick tiles of aerogel, in order to study their photon yield absorption. No significant degradation of the net Cherenkov angle resolution was observed on top of the expected 60% light yield loss effect. These preliminary results validate the CLAS12 RICH concept. Currently investigations are underway to extract final light yield and ring resolution results, to be also used for model inputs in the CLAS12 RICH simulation.

4. CLAS12 RICH Expected Performances

The CLAS12 RICH detector is simulated within the CLAS12 Geant4 framework. The description of the different optical elements is based on laboratory characterizations and the proto-

type test results above reported. The mirror geometry has been studied with ray tracing algorithms and FEM analyses and the mirror reflectivity has been assumed to follow a realistic wavelength dependence. The peculiar hybrid optics demands for a smart and robust pattern recognition algorithm even though a low multiplicity of 0.7 charged tracks per sector is anticipated for the semi-inclusive deep-inelastic scattering events of interest. The current development involves maximum likelihood methods comparing the pattern expected from direct ray tracing for the different hadron hypotheses with the recorded MA-PMT hits. The studied background accounts for secondaries from Moeller scattering off the target, the low level of MA-PMT dark counts, and the Rayleigh scattering in the aerogel radiator. The preliminary results indicate that a clear hadron separation, with a 1:500 pion rejection power, can be obtained in the full 3-8 GeV/c momentum range for scattering angles up to 25 degrees, ensuring the completion of the approved physics program.

References

- [1] CLAS12 Technical Design Report, version 5.1 208 (2008).
- [2] J. Dudek *et al.*, *Eur.Phys.J. A* **48** (2012) 187.
- [3] H. Avakian *et al.*, *arXiv:1202.1910v2 [hep-ex]* (2012)
- [4] M. Contalbrigo *et al.*, *Nucl. Instrum. Meth. A* **639** (2011) 302.
- [5] A. El Alaoui *et al.*, *Physics Procedia* **37** (2012) 773.
- [6] R. De Leo *et al.*, *Nucl. Instrum. Meth. A* **595** (2008) 19; A. Yu. Barnyakov *et al.*, *Nucl. Instrum. Meth. A* **453** (2000) 326; R. Pereira *et al.*, *Nucl. Instrum. Meth. A* **639** (2011) 37; R. Forty *et al.*, *Nucl. Instrum. Meth. A* **623** (2010) 294.
- [7] T. Iijima *et al.*, *Nucl. Instrum. Meth. A* **598** (2009) 138.
- [8] A. Yu. Barnyakov *et al.*, *Nucl. Instrum. Meth. A* **639** (2011) 225.
- [9] T. Bellunato *et al.*, *Nucl. Instrum. Meth. A* **556** (2006) 140.
- [10] T. Bellunato *et al.*, *Eur. Phys. J. C* **52** (2007) 759.
- [11] R. De Leo *et al.*, *Nucl. Instrum. Meth. A* **457** (2001) 52.
- [12] Y. Sallaz-Damaz *et al.*, *Nucl. Instrum. Meth. A* **614** (2010) 184.
- [13] R. A. Montgomery *et al.*, *Nucl. Instrum. Meth. A* **695** (2012) 326.
- [14] S. Blin *et al.*, *IEEE Nucl. Sci. Symp. Conf. Rec. 2010* (2010) 1690.